LAWRENCE
LIVERMORE
NATIONAL
LABORATORY

UCRL-JRNL-215872

Damped and thermal motion of large, laser-aligned molecules in droplet beams

D. Starodub, B. Doak, K. Schmidt, U. Weierstall, J. Wu, J. Spence, M. Howells, M. Marcus, D. Shapiro, A. Barty, H. Chapman

October 4, 2005

Journal of Chemical Physics

For J. Chem Phys. July 27 2005.

Damped and thermal motion of large, laser-aligned molecules in droplet beams.

D. Starodub,[a)] B. Doak, K. Schmidt, U. Weierstall, J. Wu, and J. Spence

Department of Physics, Arizona State University, Tempe, AZ 85287, USA

M. Howells and M. Marcus

Advanced Light Source, Lawrence Berkeley Lab, Berkeley, CA 94720, USA

D. Shapiro, A. Barty and H. Chapman

Lawrence Livermore Lab, 7000 East Ave., Livermore, CA 94550, USA.

PACS numbers: 33.80.-b, 47.55.Dz, 87.64.Bx, 87.80.Cc

Abstract.

We consider a monodispersed Rayleigh droplet beam of water droplets doped with proteins. An intense infrared laser is used to align these droplets. The arrangement has been proposed for electron and X-ray diffraction studies of proteins which are difficult to crystallize. This paper considers the effect of thermal fluctuations on the angular spread of alignment in thermal equilibrium, and relaxation phenomena, particularly the damping of oscillations excited as the molecules enter the field. The possibility of adiabatic alignment is also considered. We find that damping times in high pressure gas cell as used in X-ray diffraction experiments are short compared to the time taken for molecules to traverse the beam, and that a suitably shaped field might be used for electron diffraction experiments in vacuum to provide adiabatic alignment, thus obviating the need for a damping gas cell.

[a)] Electronic address: Dmitri.Starodub@asu.edu

1. Introduction.

This paper analyses the motion of large molecules such as proteins passing in vacuum through the field of an intense non-resonant infrared laser. The molecules may be coated with a thin ice jacket. Surplus ice from initially spherical droplets has been sublimated. We are especially interested in the thermal fluctuations and damped oscillations of the motion for a single-file stream of molecules traveling at about 50 m/sec at low temperature. X-ray and electron diffraction from such a beam has been suggested as a method for solving proteins which cannot be crystallized, and the resolution of the resulting reconstructed charge-density map has been shown to depend critically on these fluctuations and damping effects.[1] The experimental arrangement, under construction at the Advanced Light Source in Berkeley Ca, causes many doped droplets, in single file, to fall within the X-ray or electron beam at any instant. (A "shower-head" nozzle, which provides many parallel single-file streams, is also being tested). If N molecules fall within the X-ray beam at any instant, the exposure time is then given by 1/N times that for one molecule, since there is no interference (or X-ray beam coherence) between different molecules. An extensive literature exists on the doping of droplet beams[2] and on the laser-alignment of beams of small molecules.[3] Electron diffraction patterns have been obtained from a steady stream of iceballs.[4] In the previous paper[1] we discussed in detail the influence of equilibrium thermal fluctuations on misalignment, and therefore diffraction patterns from proteins. In this way equilibrium thermal fluctuations limit the sharpness of the diffraction pattern and hence the spatial resolution in the reconstruced charge-density map. (Our aim is to resolve the secondary folding structure of proteins,

which requires a resolution of about 0.7nm). Here we will concentrate on dynamic effects including damping of field-induced oscillations in a gas cell and adiabatic switch-on of a field. Both these phenomena can contribute to an improvement in the resolution of a diffraction experiment.

In this paper, we treat the simplest case, in which the molecule is considered to have two equal moments of inertia $I_x = I_y = I; \quad I_z = 0$, so that the angular momentum about its long (z)-axis may be neglected. Also, we assume that the dielectric polarizability of the molecule has uniaxial anisotropy with the easy axis coinciding with the mechanical long axis. The effect of deviations from these conditions will be considered in a subsequent paper.

2. Thermal fluctuations.

The direction of protein alignment is defined by direction of electric field in a linearly polarized light of the alignment laser, breaking the isotropy of space. As in previous work[5] we use the induced differential polarizability $\Delta\alpha(\kappa, e)$ as the source of alignment torque for a protein modeled as a homogeneous prolate dielectric ellipsoid of dielectric constant κ and eccentricity e. Since the minor semiaxes of the molecule under consideration are assumed to be equal, it has a single direction of pronounced anisotropy, and only a one-dimensional alignment is possible using a linearly polarized light. The shape anisotropy is the source of the difference in polarizability $\Delta\alpha(\kappa, e)$ along two orthogonal axes. In previous work[1] we give expressions for $\Delta\alpha$, finding that $\Delta\alpha = \gamma(\kappa, e)\, V$, where γ is a dimensionless function and V the protein volume. This classical model is appropriate to our large molecules or viruses, whose rotational energy levels are spaced

much more finely than kT. The energy of quadrupole interaction for one-dimensional alignment is $H = -C\ cos^2\theta$, where $C = 0.25\ E^2\ \Delta\alpha$. In the last expression E is the amplitude of the electric field of the laser, and θ the angle between the long axis of the molecule and the field. If the laser intensity I_0 is measured in Watt/cm^2 and $\Delta\alpha$ in nm^3, then $C = 2.1 I_0 \Delta\alpha \times 10^{-31}$ Joule.

Since the effects discussed depend strongly on molecular size, we compare a virus (TMV), a macromolecular assembly (the ribosome) and a medium sized protein (lysozyme). For tobacco mosaic virus (TMV), treated as a prolate spheroid with radii a = 300/2 nm and b = 17/2 nm, we find $\Delta\alpha\ (\kappa = 4) = 1.72V$, while $\Delta\alpha\ (\kappa = 15) = 10V$. These values of dielectric constant κ span the range of values for dry and hydrated material.[6] Measured optical constants for horseradish peroxidase protein give $\kappa = 2.34$ (dry).[7] For a large macromolecular assembly such as the ribosome, modeled with a = 17.5 nm and b = 12.5 nm, $\Delta\alpha\ (\kappa = 4) = 0.3V$ and $\Delta\alpha\ (\kappa=15) = 0.93V$. For the smaller protein Lysozyme, with a = 2.25 nm and b = 1.3nm, $\Delta\alpha\ (\kappa = 4) = 0.5V$ and $\Delta\alpha\ (\kappa = 15) = 1.6V$.

Collisions with gas molecules in the laser beam cause both thermal fluctuations in angular motion, and dissipative damping. In this section we consider only the thermal fluctuations, which persist after damping is complete, and may prevent recording of a sharp diffraction pattern. By analogy with the Langevin theory for partially aligned electrostatic dipoles in a field (extended to the case of induced dipole moments), the thermal average of the degree of misalignment may be written as

$$< \cos^2(\theta) >= \frac{\int \cos^2(\theta) \exp\left(\frac{C \cos^2(\theta)}{kT} \right) d\Omega}{\int \exp\left(\frac{C \cos^2(\theta)}{kT} \right) d\Omega} \qquad (1)$$

Here we assume two degrees of freedom (polar and azimuthal angles defining direction of the major molecule's axis in the lab frame) for one-dimensional alignment along the electric field in the linearly polarized light. We let $y = \cos(\theta)$, $x = C/kT$ (the ratio of potential to thermal energy) and $d\Omega = \sin\theta d\theta d\phi$. Then

$$\left\langle \cos^2(\theta) \right\rangle = \frac{\int_{-1}^{1} y^2 \exp(xy^2) dy}{\int_{-1}^{1} \exp(xy^2) dy}. \qquad (2)$$

This expression can be re-written in terms of the Dawson integral $F(x) = \exp(-x^2)\int_0^x \exp(t^2) dt$ as

$$\left\langle \cos^2(\theta) \right\rangle = -\frac{1}{2x} + \frac{1}{2\sqrt{x} \cdot F(\sqrt{x})}. \qquad (2a)$$

For our experiments we plan to use a 100 Watt CW fiber laser focused to about 10 micron diameter, operating at one micron wavelength in the near infrared, where amino acids show few absorption features. Then $I_0 = 1.3\times10^8$ Watt/cm^2, and taking $\Delta\alpha = 0.93V$ we have $C = 2.8\times10^{-19}$ Joule for the ribosome, whose radius is about 17 nm. With $T = 228$ K, a temperature previously measured for an evaporatively cooling droplet stream,[4] we have a ratio of potential to thermal energy $x = 90$, so that an expansion of Eq. (2a) is needed for large x, where the depth of the angular potential well C greatly exceeds kT, and the angular deviation must therefore be small. Integration by parts gives the asymptotic expansion of the Dawson integral at $x\to\infty$ in the form $F(x) = 1/2x + 1/(4x^3) + 3/(8x^5) + \ldots$ After substitution of this result into Eq. (2a) and series expansion we obtain, to second order of $1/x$, that

$$\left\langle \cos^2(\theta) \right\rangle = 1 - 1/x - 1/(2x^2) - \ldots, \qquad (2b)$$

so that, for large x, $1-1/x=\left\langle \cos^2(\theta)\right\rangle \sim 1-\left\langle \theta^2\right\rangle$. Therefore $1/x = kT/C = \left\langle \theta^2\right\rangle$, or

$$kT = \frac{1}{4}E^2\Delta\alpha\left\langle \theta^2\right\rangle \qquad (3)$$

The result agrees with equipartition theorem, applied to a harmonic oscillator in two dimensions. This expression, with energy proportional to the square of angular displacement, shows that under these small-angle conditions the molecule executes harmonic oscillations, and the problem is akin to that of the thermal fluctuations of a mirror galvanometer, for which Brownian fluctuations are observed.[8] The period of oscillation is $T_0 = 2\pi/\omega_0 = 2\pi\sqrt{I/K}$, where I is the moment of inertia and $K = 4\pi I_0\Delta\alpha/c$ is the spring constant, with c the velocity of light. With x = 90 we have $\left\langle \theta^2\right\rangle = 1/x$ or $\Delta\theta$ = 6° for the misalignment error appropriate to a large macromolecular protein assembly such as the ribosome, using a 100 Watt laser at 228 K. The alignment error $\sqrt{\left\langle \theta^2\right\rangle}$ varies as the inverse of square root of the laser power and is proportional to square root of temperature.

These small oscillations smear the diffraction patterns during the recording time, which limits the resolution in the reconstructed charge-density map. The rotational smearing also limits the accuracy with which the phase problem can be solved using iterative methods, as analyzed in detail elsewhere.[1] By combining Eq. (3) with the expression $f = \sqrt{\left\langle \theta^2\right\rangle}\cdot a$ for the resolution f expected in a reconstructed density map of a prolate spheroidal molecule of length 2a oscillating about its center of mass, we obtain

$$f = \frac{1}{2\pi b}\sqrt{\frac{3kTca}{2I_0\gamma(\kappa,e)}} \qquad (4)$$

From Eq. (4) the temperature T and laser intensity I_0 required to obtain a resolution f can be evaluated. This is shown in Fig.1, where the temperature is plotted against laser intensity for two proteins (Lysozyme and ribosome) and TMV at fixed resolution for two values of the (poorly-known) dielectric constant for each molecule. The volume of a cylinder is used to calculate the differential polarizability for TMV. The resolution chosen for the proteins, f = 0.7 nm, is sufficient to resolve the secondary structure of the proteins and so detect the locations of alpha-helices. The operating condition for our 100 W CW fiber laser focused at 10 μm (one micron wavelength) is indicated. It is seen that temperatures below the boiling point of liquid nitrogen are needed for alignment at this laser power. Reducing the waist of this laser to 5 μm results in sufficient TMV alignment at 250 K. Note that higher laser powers are possible - 1 kW fiber CW lasers are now available near one micron wavelength. As seen from Fig. 1, such a laser would allow efficient alignment for hydrated TMV and ribosome at room temperature.

3. Damping.

These thermal fluctuations are superimposed on the initial damped oscillations excited as the molecule first enters the laser field. The switch-on time of this field depends on the spatial distribution of the laser light at its focus. For the quadrupole interaction only the RMS value of the laser field is effective.[9] In section 4 we consider the possibility of adiabatic alignment. Here we apply the classical theory of damped harmonic oscillations to the protein alignment problem in order to determine if, for an abrupt non-adiabatic switch-on, the damping time can be made small compared with the exposure time for each molecule. For a beam traveling at 50 m/sec across an X-ray or electron beam of 10 microns diameter, the transit time is 200 ns.

The relaxation of the molecular orientation to the equilibrium state in an external field is described by the equation of motion

$$I\ddot{\theta} + \zeta\dot{\theta} + \frac{1}{4}E^2\Delta\alpha\sin(2\theta) = 0\,, \tag{5}$$

which includes the rotational torque $\zeta\dot{\theta}$ with friction coefficient ζ. In a harmonic approximation this equation is reduced to the standard equation for a damped harmonic oscillator

$$\ddot{\theta} + 2\lambda\dot{\theta} + \omega_0^2\theta = 0 \tag{6}$$

with $2\lambda = \zeta/I$ and $\omega_0 = \sqrt{K/I}$. For $\lambda<\omega_0$ (underdamped system), the damping time is

$$t_d = 1/\lambda, \tag{7a}$$

while for an overdamped system with $\lambda>\omega_0$ the damping time is equal to

$$t_d = 1\Big/\left(\lambda - \sqrt{\lambda^2 - \omega_0^2}\right). \tag{7b}$$

The damping time can be adjusted by passing the molecular beam through a medium with varying viscosity (damping cell). We note in particular that this time is proportional to viscosity in the overdamped case (where inertia is negligible, as for terminal velocity problems), but is inversely proportional to viscosity for underdamped systems, where increased viscosity reduces time to equilibrium. Fig. 2 shows this behavior for damping time against viscosity, assuming that the rotational friction coefficient depends on viscosity linearly with the same coefficient over the interval of viscosity change. Optimum extinction of oscillations is achieved in the vicinity of conditions for critical damping.

Viscosity is independent of pressure over a wide pressure range, where the mean-free-path l of the gas molecules is small compared to the characteristic macromolecule

dimension A, such that $l << A$ ($l \sim 100$ nm for air at STP). In the opposite limit of the molecular free flow (Knudsen) regime, when $l >> A$, viscosity is a function of pressure. Because in this regime the mean free path is large compared to the protein size, gas molecules scattering on the protein will not perturb the Maxwell velocity distribution in gas. Therefore, the frictional torque, experienced by a macromolecule, can be easily calculated by integrating over its surface the moment of momentum transferred to the macromolecule by impinging and scattered gas molecules. We performed this integration in linear approximation for a cylinder with circular base, approximating a TMV molecule, and for a sphere to model frictional torque experienced by Lysozyme and ribosome. For a cylinder, the rotational friction coefficient is

$$\zeta = \frac{\pi}{32} mn\bar{v}dL^3 \cdot s + \frac{\pi}{24} mn\bar{v}dL^3 \cdot (1-s), \qquad (8a)$$

where d is the cylinder diameter, L its length, m the mass of a gas molecule, and n the gas molecules concentration. The average velocity of the gas molecules is $\bar{v} = \sqrt{8kT/\pi m}$. Finally, s denotes the fraction of gas molecules, which undergo diffuse scattering, and (1 - s) is a fraction of molecules, experiencing specular scattering. This expression can be compared with that for the rotational friction coefficient in the case of a rod with a square base (specular reflection $s = 0$):

$$\zeta = \frac{1}{6} mn\bar{v}bL^3, \qquad (8b)$$

where b is the square side, and L the rod length. Equation (8b) immediately follows from the treatment of Brownian motion for a flat disk in the Knudsen regime given by Uhlenbeck and Goudsmidt.[8] For a sphere we have the result, first obtained by Epstein[10]

$$\zeta = \frac{2\pi}{3} mn\bar{v}R^4 \cdot s\,, \tag{8c}$$

where R is the radius of the sphere. In all these cases, rotational torque due to friction is proportional to gas pressure.

In a liquid and a dense gas with $A >> l$ the frictional torque experienced by a rod-like particle is[11]

$$\zeta = \frac{8\pi\eta a^3}{3\left(\ln\frac{2a}{b} - \gamma\right)}\,. \tag{9a}$$

Here a is the particle half-length, b the half-width, η the viscosity of the liquid, and $\gamma = 1.57 - 7\cdot\left(\ln^{-1}\frac{2a}{b} - 0.28\right)^2$. If the particle is approximated by a prolate spheroid with $a >> b$, then $\gamma = 0.5$.[12] Finally, the simple Stokes expression

$$\zeta = 8\pi\eta a^3 \tag{9b}$$

can be used for a sphere.

We wish to determine the conditions of pressure and viscosity needed to ensure that the damping times are much less than the transit time for a non-adiabatic entry of the proteins into the laser field. Table 1 summarizes calculated values of the damping constant $2\pi/\lambda$ for TMV, ribosome and Lysozyme in water and dry nitrogen, the latter for the free molecular regime and dense gas, using Eqs. (8) and (9). The experimental values for the damping constant in water for TMV and Lysozyme are also given. They are extracted from the diffusivity data[13] using the Einstein relationship between rotational diffusion D and friction coefficient $\zeta D = kT$. These values for the damping constant should be compared with the period of free oscillation of the molecules in the electric field of a 100 W laser focused at 10 μm diameter. We see that the motion is always

strongly overdamped in water, preventing satisfactory alignment of a molecule rotating inside a water droplet, during the transit time through the laser beam, since there is insufficient time for the alignment to occur within the allowed 200 ns. Using Eq. (7b), we find that the damping times in water are 374 ns for TMV, 124 ns for ribosome, and 72 ns for Lysozyme, all of which are too large for the transit time of 200 ns. Therefore, slower droplets (~ 5 m/s) must be used to provide alignment in water. By contrast, the oscillations are underdamped in rarified gas, again resulting in large damping times of 414 ns, 620 ns, and 67 ns at 10^4 Pa for TMV, ribosome, and Lysozyme, respectively. However, increasing the pressure in a gas damping cell to 10-50 bar allows the transition from strongly underdamped oscillations to nearly critical damping, which is optimal for the alignment of a molecule within a thin ice jacket, rotating as a solid object. When condition for critical damping is satisfied, the relaxation times are 3.7 ns, 1.8 ns, and 0.14 ns for TMV, ribosome, and Lysozyme, respectively. These values are small as compared to the transit time through laser beam.

All three damping regimes are demonstrated in Fig. 3, which compares the damping behavior of TMV in a gas cell at two pressures of 10^4 and 10^6 Pa (possible for a medium or hard X-ray diffraction experiment) with that of TMV in liquid water droplets. The presented curves are produced by numerical integration of Eq. (5) with parameters from Table 1, using the fourth-order Runge-Kutta method. We see that damping times in water are prohibitively long compared to the transit time at the droplet velocity of 50 m/s. One should note, however, that provided there is no time limitation as in our case, alignment in liquid can still be achieved in (quasi-) static regime. It is interesting that experiments were successful in aligning TMV in water in a static electric field as early as

1950.[14] Recently the possibility to control motion of a large rodlike particle (3.8 μm long glass nanorod) by applying light torque (laser wrench) has been demonstrated.[15] Well above atmospheric pressure, the possibility of critical damping is predicted.

4. Adiabatic conditions.

If the rise-time of the laser intensity experienced by the passing molecule is sufficiently slow, the initial overshoot of the molecular motion will be reduced, and gas damping may not be needed. In this section we investigate the possibility of obtaining this desirable adiabatic condition. In an open system with a slowly-varying characteristic parameter (laser intensity in this case) the area enclosed by a system trajectory in phase space is an adiabatic invariant.[16] For a harmonic oscillator with time dependent spring constant $K = K(t)$ the conserved quantity is $E(k)/\omega(k)$, where $E(k)$ is the energy of a system, and $\omega(k)$ the oscillator frequency. Then the amplitude of oscillation is proportional to $K(t)^{-1/4}$, and can be made small if the laser intensity rise-time is slow enough. Therefore, the experimental requirements for a gas-filled damping cell above near atmospheric pressure to achieve proper alignment could be eliminated, or at least relieved, if the initial rotation of the molecule occurs sufficiently slowly to ensure adiabatic conditions in which the molecule remains instantaneously in equilibrium with the applied, slowly varying field. The requirement for this is that the switch-on time of the field greatly exceeds the natural period of oscillation of the molecule T_0. That this is certainly possible is indicated in Table 1, where the transit time is 200 ns for a 10 micron laser focus. The switch-on time of the laser may be controlled either by spatial shaping of the field using the focusing lens or by adjusting the molecule velocity. For the smallest protein and molecule velocity of 50 m/s from Table 1 we evidently require that the field rise to its maximum value over a

distance greater than (0.90/200)×10 = 0.045 microns, which is much less than the value expected for a Gaussian beam. On the other hand, for a Gaussian beam, the time required to reach an acceptably small amplitude of oscillation may be too large as compared to sharper beams, and may not compensate for the overall better alignment in the center of a Gaussian beam. So we may then have the opposite problem - to make the edges of the laser beam sharp enough. The optimum conditions for the beam profile should be determined, such that a molecule in the laser beam achieves a reasonably good alignment in a reasonably short time, which is small compared to the exposure time.

In order to determine the conditions for adiabatic alignment, we numerically solve Eq. (5) with $\zeta = 0$ for a particle traversing a laser beam with an intensity profile described by

$$I(r) = \begin{cases} I_0, r \le r_0 \\ I_0 \cdot 2^{-\frac{(r(t)-r_0)^2}{r_{1/2}^2}}, r > r_0 \end{cases}, \qquad (10)$$

where r_0 defines the radius of the central area with uniform intensity, $2 \cdot r_{1/2}$ is the FWHM for the Gaussian edge of the beam, and the normalization constant I_0 is defined by a laser power of 100 W. The value of $r_{1/2} = 0$ corresponds to an abrupt non-adiabatic switch-on, and $r_0 = 0$ is the slowest intensity rise-time achieved for Gaussian profile. At $r_{1/2} = 0$ (sharp edge) the value chosen for r_0 was 5 micron (the laser focused on the spot with a diameter of 10 micron). The Runge-Kutta method was employed for integration. It was tested by comparing the numerically calculated trajectory with the closed-form solution of the problem, obtained for a Lorentz distribution.[17] Fig. 4(a) shows the motion of a large heavy (40.5×10^6 Da) TMV particle for the laser profiles with (1) abrupt edges, (3) Gaussian shape, and (2) intermediate edge sharpness. For the non-adiabatic condition (1)

the molecule undergoes violent oscillations with amplitude equal to the angle at which it enters the beam. But even a minor smearing of the beam edge results in a dramatic drop of the particles oscillation amplitude within the beam (curve 2). Further smearing of the beam edges slowly reduces the oscillation amplitude to its minimum value. The adiabatic conditions can also be modified by changing the molecule velocity for a given laser beam profile, as shown in Fig. 4(b). Here the small protein Lysozyme passes through a Gaussian beam with different velocities, and the molecular alignment (which can be better than a few degrees) is significantly affected by the particle velocity. These data are summarized in Fig. 5, which presents the degree of alignment in the center of the laser focus as a function of the field intensity switch-on time $r_{1/2}/v$, where v is the particle velocity. The data can be fitted by a power law, with a power of ~ -0.45. The alignment angle is about 4 times larger for TMV as compared to lysozyme under similar conditions, and this ratio slowly increases for larger values of $r_{1/2}/v$. In the case of TMV, in order to confine the molecule misalignment within 5°, the time of flight through the region with rising laser intensity must be 600 ns, while for lysozyme a misalignment of 2° is achieved already at an entry time of 100 ns. The one-dimensional model described above does not take into account the angular momentum about the molecular long axis. The gyroscopic effects of this angular inertia result in an effective potential, confining the molecule motion between two polar angles θ_{min} and θ_{max}. For thermal energies small compared to the potential of the molecule quadrupole interaction with the electric field, this effective potential approaches the shape of the quadrupole interaction potential, and has an additional pole at $\theta = 0$. Thus the problem can be reduced to a one-dimensional rotation about the field direction, however with $\theta_{min} \approx 0$. Numerical integration of the equation of

motion in the θ coordinate shows that the one-dimensional approximation, applied in this paper, satisfactorily describes free oscillations of TMV in a laser electric field even at room temperature, while for lysozyme deviations from a three-dimensional behavior become small only at very low temperatures. A complete treatment of a 3D adiabatic alignment, taking into account the rotational friction and thermal fluctuations, will be described in a subsequent paper.

5. Discussion and conclusions.

Since the interaction energy of the particle with the laser beam is proportional to $\cos^2\theta$ for this simple one-dimensional case, the restoring force is zero for $\theta = 90°$, and an inverted molecule has the same energy as an erect one. In general laser alignment is sensitive to the direction but not the sense of the three molecular axes, and laser alignment of this type (containing a mixture of molecular orientations in the beam for a molecule with no symmetry) has been achieved by several groups using elliptically polarized laser light. The result will be to introduce spurious mirror planes of symmetry due to two-fold rotation about these axes into the two-dimensional diffraction pattern, in addition to the inversion symmetry of all single-scattering patterns (Friedel's law). It has been suggested that this degeneracy may be removed by the addition of a weak DC external field, which interacts with the linear Stark permanent dipole term. In this way the absolute orientation of small molecule has been fixed in space recently by laser alignment.[18]. We are also currently investigating the possibility that absolute alignment may not be needed. Since proteins consist of just 20 amino acids of known structure and (usually) sequence, for which the bond angles and lengths are known, the addition of this

a-priori information may allow the phase problem to be solved using diffraction data containing these spurious mirror planes.[19]

We find that the damping times in high pressure gas cell to be used in our X-ray diffraction experiments can be made short compared to the time taken for molecules to traverse the beam, and that a suitably shaped laser field might be used for electron diffraction experiments in vacuum to provide adiabatic alignment, thus obviating the need for a damping gas cell.

Acknowledgements.

The authors are grateful to Prof T. Seideman and Dr. G. Hembree for valuable comments. This work was supported by an NSF STC award to the Center for Biophotonics at UC Davis under cooperative agreement PHY 0120999 and NSF SGER award DBI-0429814.

This work was performed under the auspices of the U.S. Department of Energy by University of California, Lawrence Livermore National Laboratory under contract W-7405-Eng-48.

References

[1]J. C. H. Spence, K. Schmidt, J. S. Wu, G. Hembree, U. Weierstall, B. Doak, and P. Fromme, Acta Cryst. **A61**, 237 (2005).

[2]A. Lindinger, J. P. Toennies, and A. F. Vilesov, J. Chem. Phys. **110**, 1429 (1999).

[3]T. Seideman, J. Chem. Phys. **115**, 5965 (2001).

[4]L. S. Bartell and J. Huang, J. Phys. Chem. **98**, 7455 (1994).

[5]H. Stapelfeldt and T. Seideman, Rev. Mod. Phys. **75**, 543 (2003).

[6]T. Simonson, Rep. Prog. Phys. **66**, 737 (2003).

[7]E. T. Arakawa, P. S. Tuminello, B. N. Khare, and M. E. Milham, Biospectroscopy **3**, 73 (1997).

[8]G. Uhlenbeck and S. Goudsmit, Phys. Rev. **34**, 145 (1929).

[9]B. Friedrich and D. Herschbach, J. Chem. Phys. **99**, 15686 (1995).

[10]P. S. Epstein, Phys. Rev. **23**, 710 (1924).

[11]S. Broersma, J. Chem. Phys. **32**, 1626 (1960).

[12]F. Perrin, J. Phys. Radium **5**, 497 (1934).

[13]D. Brune and S. Kim, Proc. Nat. Acad. Sci. **90**, 3835 (1993).

[14]C. T. O'Konski and B. H. Zimm, Science **111**, 113 (1950).

[15]W. A. Shelton, K. D. Bonin, and T. G. Walker, Phys. Rev. E **71**, 036204(2005).

[16]L. D. Landau and E. M. Lifshitz, *Mechanics*, 3rd edition, (Butterworth-Heinemann, Oxford, 2003

[17]L. Marton, Rep. Prog. Phys. **10**, 204 (1944).

[18]H. Sakai, S. Minemoto, H. Nanjo, and T. Suzuki, Phys. Rev. Lett. **90**, 083001 (2003).

[19]S. H.W.Scheres and P. Gros, Acta Cryst. **D57**, 1820 (2001).

Molecule	Period, ns	Damping constant, ns				Transit time, ns
		N_2, $l<<a$, $s = 1$	N_2, $l>>a$	Water, theory	Water, experiment	
TMV, l = 300 nm, r = 8.5 nm, γ = 10	23	$2.6\times10^7/P$	26	0.45	0.51	200
Ribosome, r = 17.5 nm, γ = 0.93	11	$3.9\times10^7/P$	18	0.31	-	200
lysozyme, r = 1.9 nm, γ = 1.6	0.90	$4.2\times10^6/P$	0.21	3.6×10^{-3}	3.9×10^{-3}	200

Table I. Values of the oscillation period, damping constant in water and gas (nitrogen in the limits of Knudsen and dense gas), and transit time for two proteins and TMV, assuming a 100 Watt IR laser with 10 micron focus. A pressure unit is *Pa*.

FIG. 1. Alignment temperature vs laser intensity for a protein (dot line), macromolecule (dash line) and virus (solid line) at the misalignment values indicated. Two values of the dielectric constant are shown, which span the range from dry (smaller) to hydrated (larger value) material. The resolution f is 0.7 nm for lysozyme and ribosome, and 1 nm for TMV.

FIG. 2. Sketch of damping time against viscosity, with transit time indicated.

FIG. 3. Comparison of damping behavior of TMV in water (overdamped regime) and nitrogen gas at lower (underdamping) and higher (critical damping) pressures. The damping time exceeds the transit time for water and nitrogen at lower pressure.

FIG 4. Dependence of a particle trajectory on adiabatic conditions for (a) TMV crossing the laser beam with various shapes, (b) lysozyme in the Gaussian beam with various travel velocity. In all cases, a molecule enters the beam at the angle of 45° at zero angular velocity.

FIG. 5. Amplitude of the molecule oscillation in the center of laser beam as a function of entry time. Solid squares (for lysozyme) and open circles (TMV) result from numerical integration of equation of motion, and lines are the least-square linear fit. Laser power is 100 W.

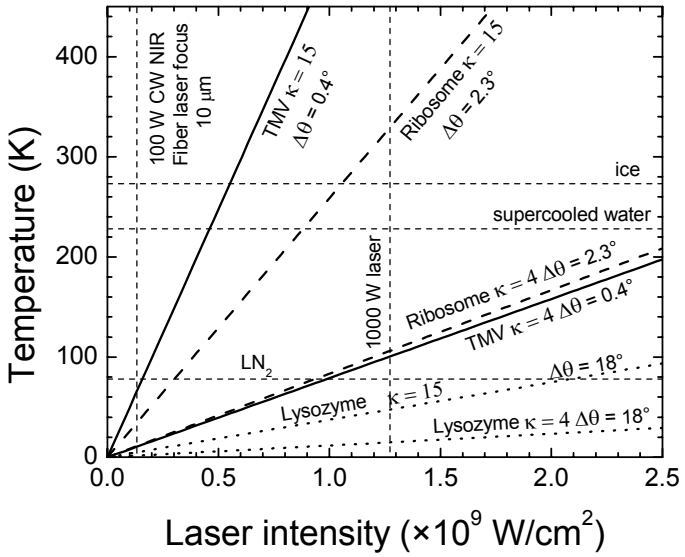
Temperature (K)
Laser intensity (×10^9 W/cm^2)
100 W CW NIR
Fiber laser focus
10 μm
1000 W laser
TMV κ = 15
Δθ = 0.4°
Ribosome κ = 15
Δθ = 2.3°
ice
supercooled water
Ribosome κ = 4 Δθ = 2.3°
TMV κ = 4 Δθ = 0.4°
LN2
Δθ = 18°
Lysozyme
κ = 15
Lysozyme κ = 4 Δθ = 18°
0
100
200
300
400
0.0
0.5
1.0
1.5
2.0
2.5

FIG. 1.

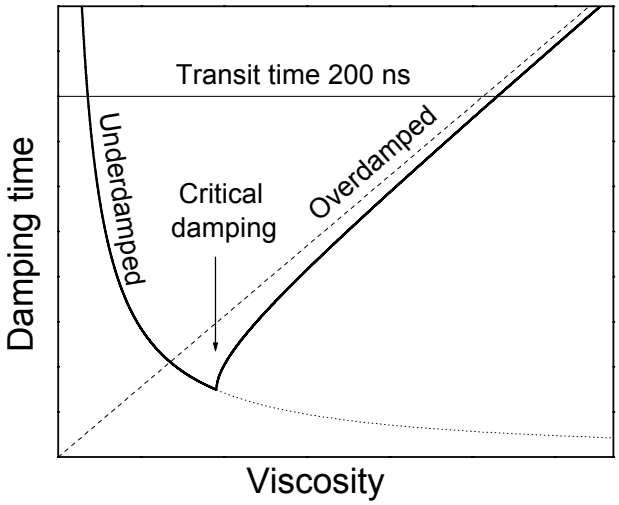
Transit time 200 ns
Underdamped
Critical
damping
Overdamped
Damping time
Viscosity

FIG. 2.

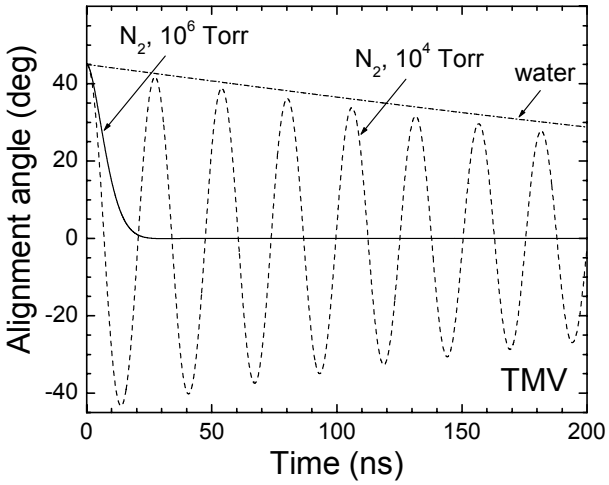
N2, 10^6 Torr
N2, 10^4 Torr
water
TMV
Alignment angle (deg)
Time (ns)
40
20
0
-20
-40
0
50
100
150
200

FIG. 3.

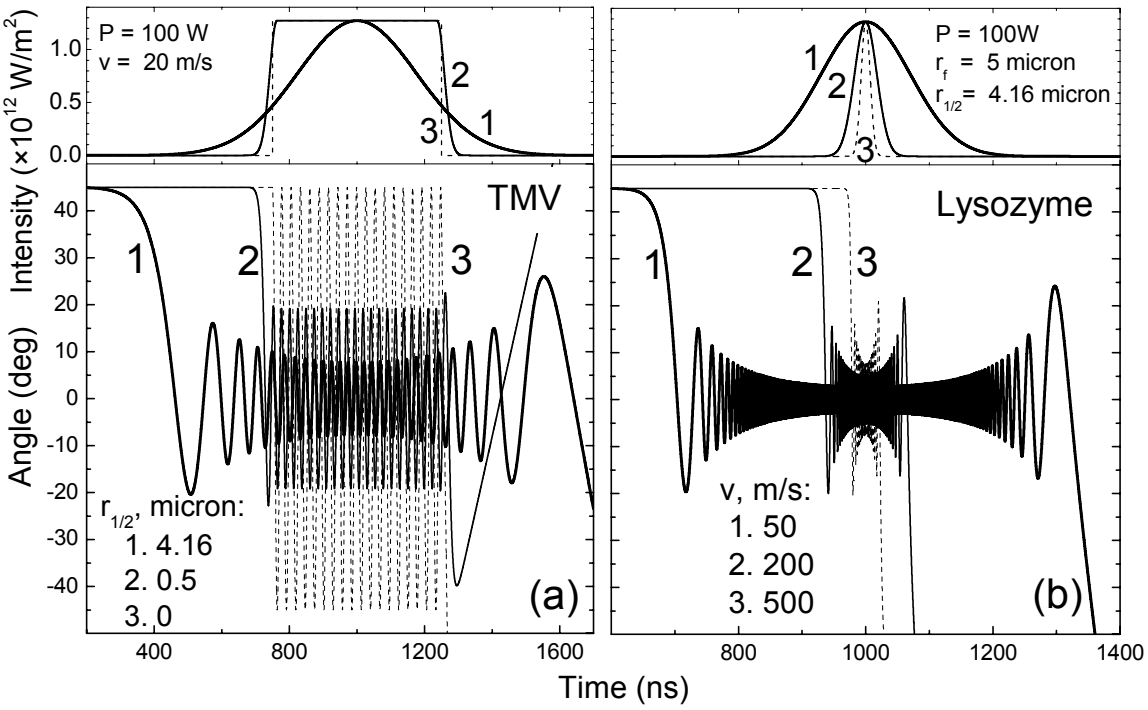
P = 100 W
v = 20 m/s
P = 100W
r_f = 5 micron
r_1/2 = 4.16 micron
Intensity (×10^12 W/m^2)
Angle (deg)
TMV
Lysozyme
r_1/2, micron:
1. 4.16
2. 0.5
3. 0
v, m/s:
1. 50
2. 200
3. 500
(a)
(b)
Time (ns)

FIG. 4

.

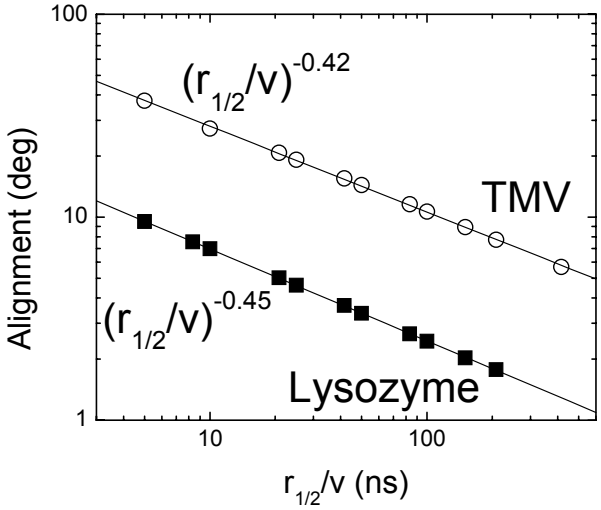
100
10
1
Alignment (deg)
$(r_{1/2}/v)^{-0.42}$
TMV
$(r_{1/2}/v)^{-0.45}$
Lysozyme
10
100
$r_{1/2}/v$ (ns)

FIG.5.